


 Cite this: *RSC Adv.*, 2021, 11, 30961

Experimental and kinetic study of the conversion of waste starch into glycolic acid over phosphomolybdic acid

 Yongzhen Qiao,^{ab} Xiu Wang^{ab} and Hongqi Dai^{ab} 

The starch used to enhance the paper surface dissolves in water during the production process and forms pollutants that accumulate in water when old corrugated cardboard (OCC) is returned to a paper mill for pulping and reuse. At present, anaerobic fermentation is widely used in the paper industry to treat starch-containing wastewater, producing biogas energy, or oxidative decomposition, which is a huge waste of valuable starch resources. Phosphomolybdic acid (PMo₁₂) is a highly selective catalyst for the oxidation of carbohydrates; therefore, PMo₁₂ can be envisaged as a suitable catalyst to convert waste starch into glycolic acid, an important high added-value chemical. In this paper, the catalytic oxidation technology of PMo₁₂ was explored to produce glycolic acid from starch contained in OCC papermaking wastewater, and the kinetics and influencing factors of the catalytic oxidation reaction were studied. The results indicated that the PMo₁₂-catalyzed oxidation of starch followed a first-order reaction; the reaction rate constant increased with increasing the temperature, the apparent activation energy of starch to monosaccharide was 104.7 kJ mol⁻¹, the apparent activation energies of starch and monosaccharide to humins were 126.5 and 140.5 kJ mol⁻¹, and the apparent activation energy of monosaccharide to glycolic acid was 117.2 kJ mol⁻¹. The yields of monosaccharide and glycolic acid were 80.7 wt% and 12.9 wt%, respectively, and the utilization of starch resources was about 90.0 wt% under the following reaction conditions: temperature, 145 °C; reaction time, 120 min; pH, 2. Therefore, the feasibility of the PMo₁₂-catalyzed oxidation of starch to produce high value-added glycolic acid is demonstrated, which has theoretical guiding significance and potential application value for the clean production and resource utilization of waste starch in the OCC papermaking process.

 Received 3rd August 2021
 Accepted 10th September 2021

DOI: 10.1039/d1ra05890h

rsc.li/rsc-advances

1. Introduction

Starch is a rich and sustainable natural resource.¹ It is not only a source of energy for human survival but also an important raw material for the food processing industry, paper industry, textile industry, and adhesive production, among other fields. Owing to its low cost and green degradability, starch is often used as a surface strengthening agent in the production of corrugating medium and cardboard.² However, when the old corrugated cardboard (OCC) waste paper is recycled and repulped, the paper fibers are dissociated, which results in the release and dissolution of a large amount of starch into the water, becoming a source of pollution. The accumulation of starch to a certain extent can seriously affect the paper production environment, the stable operation of the system, and the product quality. In addition, a large number of microorganisms can also multiply

and rot, which produces a very bad smell and is detrimental to the production system and the environment. According to the report of China's paper industry in 2019, China's consumption of corrugating medium and cardboard was 44 million tons. On the basis of the usual content of starch as surface sizing agent per ton of paper, which is 40–60 kg, 176 000–264 000 tons of starch that cannot be recycled will be dissolved in OCC pulping wastewater, resulting in a great waste of food resources.^{3,4} At present, most of the starch-containing wastewater produced by the OCC wastepaper repulping process is treated by anaerobic fermentation to produce biogas energy.^{5,6} However, the biological treatment of starch wastewater requires special equipment, covers a large area, and offers low resource utilization. Therefore, the development of a method for the efficient utilization of waste starch (WS) is a pressing concern.

Glycolic acid is an important chemical product and organic synthesis intermediate, which contains a hydroxyl group and a carboxyl group, exhibiting the properties of both an alcohol and an organic acid. It is widely used in dyeing, personal care products, metal cleaning, adhesives, and textiles, especially in polymer degradation materials and pharmaceutical engineering materials.^{7–10} In nature, glycolic acid mainly exists in

^aJiangsu Co-Innovation Center of Efficient Processing and Utilization of Forest Resources, Nanjing Forestry University, Nanjing, China, 210037. E-mail: hgdhq@njfu.edu.cn

^bInternational Innovation Center for Forest Chemicals and Materials, Nanjing Forestry University, Nanjing, China, 210037



sugarcane, sugar beet, and immature grape juice, albeit in low content. In addition, it is difficult to purify from these natural sources. In industrial production, chemical synthesis is the most commonly used method to prepare glycolic acid; however, the water and energy consumption is high, which results in a huge waste of water resources and energy. Hence, chemical conversion of biomass to produce glycolic acid can be envisaged as a reasonable and effective alternative to the traditional chemical synthesis.¹¹ In recent years, researchers have focused on the direct conversion of biomass into glycolic acid to realize the utilization of biomass stemming from agricultural and forestry waste.^{12–14} For example, niobium-supported silica¹⁵ and basic hydrotalcites¹⁶ have been used to obtain glycolic acid from cellulose. However, this transformation requires a long contact time (>24 h), which hinders its industrial application. Therefore, the development of an efficient and green preparation of glycolic acid is a great research challenge.

For the catalytic transformation of biomass, polyoxometalates (POMs) have been recently shown to exhibit unique advantages.^{17–19} Thus, the Brønsted and Lewis acid properties of POMs have important application in the hydrolysis and transformation of natural polysaccharides including cellulose and starch. Hydrolytic transformations such as the hydrolysis of cellulose to glucose can be promoted by Brønsted acid sites, whereas Lewis sites enable glycolytic transformations, *e.g.*, retro-aldol reaction, and oxidation transformations. Silica- and alumina-supported phosphotungstic acid and silicotungstic acid can catalyze the conversion of cellulose into glycolic acid, but the highest yield is as low as 4.2%.²⁰ By contrast, molybdenum (Mo)-based Keggin-type POMs exhibit high catalytic efficiency. POMs containing Mo can be effectively dispersed in water medium to realize the conversion of polysaccharides into glycolic acid. In this process, the monosaccharides obtained by hydrolysis of natural

polysaccharides undergo two consecutive retro-aldol reaction yielding three molecules of glycolaldehyde, which is the main intermediate. These molecules are then oxidized to glycolic acid.^{12,21} Starch is easier to depolymerize than cellulose or lignocellulosic feedstock.²² Therefore, the oxidation of starch to glycolic acid catalyzed by Mo-based POMs such as phosphomolybdic acid ($\text{H}_3\text{PMo}_{12}\text{O}_{40}$, here denoted as PMo_{12}) has great application potential.

Motivated by this background, we have developed a PMo_{12} -catalyzed oxidation and degradation of WS from OCC pulping process water to glycolic acid (Fig. 1). This paper describes the method and the investigation of the factors influencing the kinetics of the oxidation and degradation of WS by PMo_{12} . Furthermore, on the basis of the experimental results, the kinetic model of the PMo_{12} -catalyzed oxidation degradation of WS to glycolic acid is established, which provides a reference and theoretical basis for the clean production of papermaking and the utilization of starch resources in wastewater.

2. Materials and methods

2.1 Materials

OCC pulping wastewater was provided by Nine Dragons Paper Co., Ltd. (Taicang, China). PMo_{12} was supplied by Shanghai Aladdin Chemicals Co., Ltd. (Shanghai, China). Phosphoric acid (AR), cesium chloride (CsCl, AR), and sodium hydroxide (NaOH, AR) were purchased from Sinopharm Chemical Reagent Co., Ltd. (Shanghai, China).

2.2 Pretreatment of OCC pulping wastewater

The wastewater from a multidisc thickener in the OCC waste paper re-pulping process was filtrated using a Busher funnel with 325 mesh. Then, the filtrate was centrifuged at 4500 rpm for 20 min using a high-speed centrifuge. The supernatants

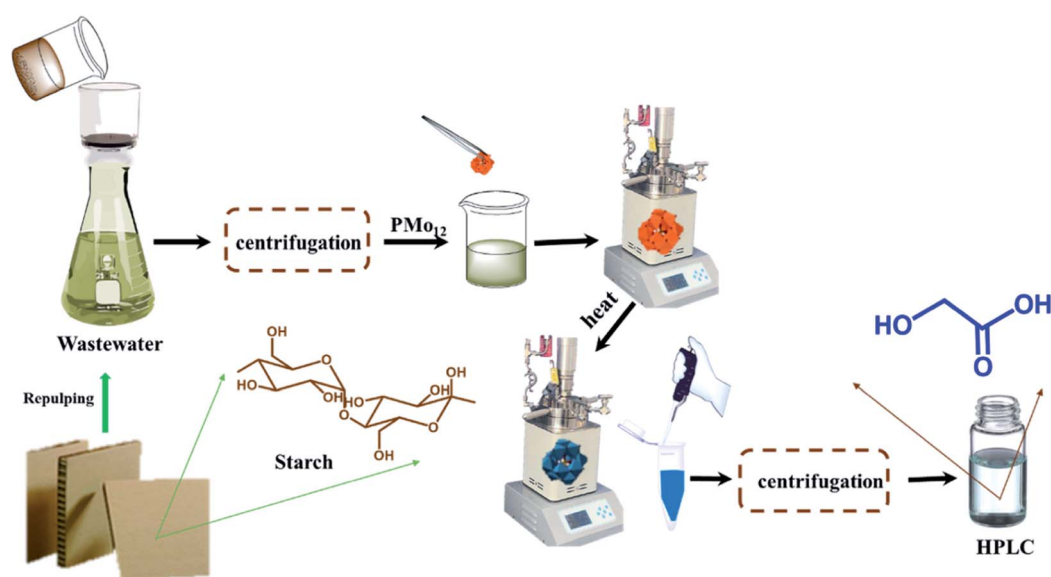


Fig. 1 Schematic diagram of phosphomolybdic acid catalyzed degradation of waste starch.



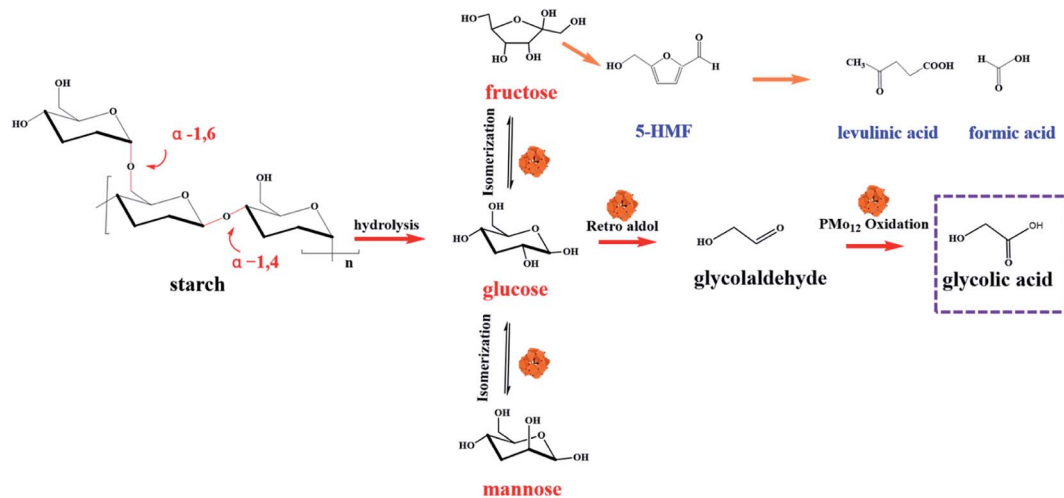


Fig. 2 The proposed reaction mechanism in the degradation of waste starch with PMo_{12} .

were subsequently placed in a dialysis bag with MWCO 8000–12 000 (Da) to obtain a water-soluble organic solution containing WS and water-soluble organic matter without inorganic substances. The content of WS in the OCC pulping wastewater was determined to be about 5 g L^{-1} according to an amylase method and high-performance liquid chromatography (HPLC) analysis.³

2.3 Hydrothermal reaction of WS with PMo_{12}

A 200 mL miniature magnetic reaction kettle was used in this experiment. The OCC wastewater was treated before the reaction and concentrated by rotary evaporation to increase the concentration of WS. To prepare the reaction solution, PMo_{12} (20 wt% relative to the mass of starch) was added to 100 mL of OCC pulping wastewater. The pH of 20 wt% PMo_{12} in 100 mL wastewater was 2.8. Then, the pH of wastewater was adjusted to 1 and 2 by phosphoric acid. Moreover, the pH was turned from 2.8 to 4 by 1 M sodium hydroxide solution. The resulting solution was poured into the reactor to perform the catalytic oxidation. The air in the reactor was removed by passing a N_2 flow to reduce the interference of oxygen, the required temperature was adjusted, and the stirring speed was set to 300 rpm. When the temperature reached the experimental temperature, the reaction was started and then stopped by cooling the reactor in an ice water bath immediately after a certain period of time. Three parallel assays were performed for each experiment.

2.4 Product treatment and analysis methods

A stoichiometric amount of CsCl was added to the solution after the hydrothermal reaction. The PMo_{12} catalyst that precipitated immediately was removed by centrifuging at 5°C and 10 000 rpm for 10 min in a high-speed low-temperature centrifuge, followed by filtering through a $0.22 \mu\text{m}$ nylon filter membrane to ensure that there was no particle residue in the sample. The treated samples were analyzed by HPLC using an Aminex BioRad-HPX-87H column and a refractive index

detector. The yields of monosaccharide and glycolic acid were calculated according to eqn (1) and (2) as follows:

$$\text{Monosaccharide}(\text{wt}\%) = \frac{\text{monosaccharide}(m_1)}{\text{starch}(m)} \times 100\% \quad (1)$$

$$\text{Glycolic acid}(\text{wt}\%) = \frac{\text{glycolic acid}(m_2)}{\text{starch}(m)} \times 100\% \quad (2)$$

3. Results and discussion

3.1 Analysis of the PMo_{12} -catalyzed oxidative degradation of starch

PMo_{12} has both mild acidity and oxidation ability and can maintain good catalytic activity and high stability during the processes of biomass hydrolysis, isomerization, and retro-aldol reaction, which renders it suitable for the oxidation of polysaccharides such as cellulose and starch to organic acids.^{23–25} So far, few studies have described the use of PMo_{12} as an oxidation catalyst for starch conversion. In the hydrothermal reaction, PMo_{12} first uses H^+ generated by ionization to cleave the α -1,4- and α -1,6-glycosidic bonds between starch molecular chains to form monosaccharides (Fig. 2). Second, PMo_{12} catalyzes the cleavage of the carbon bond of the monosaccharides through an electron transfer and oxygen transfer mechanism.²⁶ Moreover, starch likely undergoes cleavage reaction affording the hydrolysate monosaccharides, which contains glucose, mannose and fructose. The Mo in PMo_{12} is considered to be equipped with a dual function of sugar conversion. Isomerization and retro-aldol reaction are conducted by PMo_{12} , thus the aldohexose (glucose to mannose) is generated during the process. Finally, glycolaldehyde that created from glucose and mannose by retro-aldol reaction is oxidized to glycolic acid.^{12,21} According to this mechanism, PMo_{12} provides both electrons and oxygen atoms to cleave single C–C bonds and form oxygen-containing products.

To gain insight into the degradation rate of the catalytic oxidation of WS by the PMo_{12} catalyst, various conditions



Table 1 Analysis of the phosphomolybdic acid catalyzed oxidative degradation of starch

T (°C)	Products			
	Monosaccharide (wt%)	Glycolic acid (wt%)	5-HMF (wt%)	Formic acid (wt%)
140	61.5 ± 2.2	8.0 ± 1.4	0.8 ± 0.1	0
145	66.1 ± 2.2	16.5 ± 0.9	1.1 ± 0.2	0.026
150	57.0 ± 1.1	15.7 ± 1.0	1.2 ± 0.1	0.049
160	25.8 ± 2.2	15.8 ± 1.0	3.0 ± 0.1	0.011

including reaction temperature, PMo_{12} dosage, reaction time, starch concentration, and pH were examined. The results summarized in Table 1 show that the Mo-containing catalyst was effective for the conversion of polysaccharides. Monosaccharide and glycolic acid were the main products, which were obtained with high selectivity. The strong acidity of PMo_{12} was beneficial to the hydrolysis of starch, while its moderate oxidation ability was beneficial to the selective oxidation of aldehyde groups in the degradation products. The continuous cascade of retro-aldol reaction caused the cleavage of the monosaccharides from starch hydrolysis, which improves the high selectivity for glycolic acid. Meanwhile, during the catalytic oxidation of PMo_{12} , a series of byproducts were obtained, including soluble 5-HMF, formic acid and insoluble brown matter, which can be regarded as humins.²⁷ Horvat *et al.* suggested that the 5-HMF produced at high temperature would further decarboxylate to form levulinic acid and formic acid,

and could also lead to polymerization reactions producing humins.²⁸ The total yield of the products in the whole reaction process was less than 100%, which may be caused by the decomposition of the degradation products into CO_2 , H_2 , CO , and H_2O at the present high temperature and acidic conditions.²⁹

3.2 Effect of the starch concentration on the starch degradation products

To study the effect of the starch concentration on its catalytic degradation, the amount of the PMo_{12} catalyst was set to 20 wt% of the starch concentration, the temperature of the reaction system was fixed at 150 °C, the reaction products were analyzed at the reaction time of 60, 120, 180, 240, and 300 min, and the starch concentration was varied at 2.5, 5, 12.5, and 20 g L^{-1} . As can be seen in Fig. 3a, for a starch concentration of 2.5 g L^{-1} , the

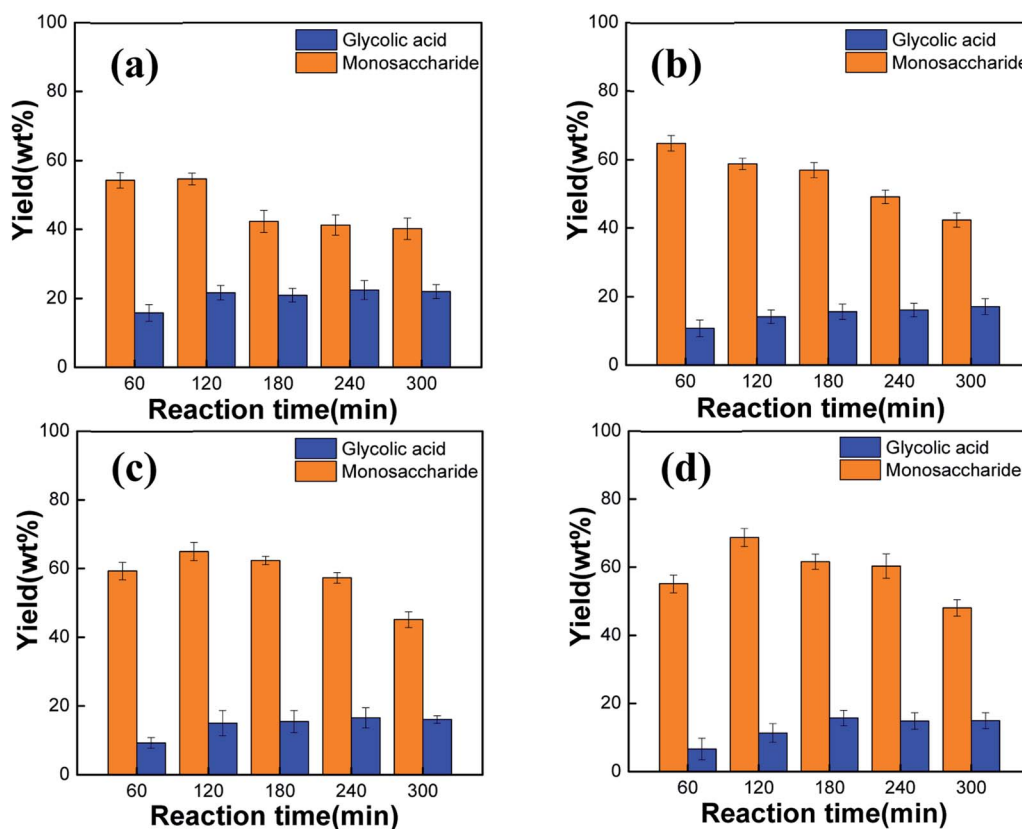


Fig. 3 Effect of the starch concentration on the yield of the starch degradation products: (a) 2.5 g L^{-1} ; (b) 5 g L^{-1} ; (c) 12.5 g L^{-1} ; (d) 20 g L^{-1} .



yield of monosaccharide decreased gradually, being the highest yield 54.7 wt% at 120 min, and the yield of glycolic acid increased first until reaching a maximum of 22.5 wt% at 240 min and then decreased. Fig. 3b shows that for a starch concentration of 5 g L^{-1} , the yield of monosaccharide decreased gradually from the maximum yield of 64.8 wt% at 60 min up to a yield of only 42.3 wt% at 300 min, and the maximum yield of glycolic acid reached 17.1 wt% after 300 min of reaction. For a starch concentration of 12.5 or 20 g L^{-1} , the starch was not completely hydrolyzed at the beginning of the reaction, and the monosaccharide yield increased first and then decreased, reaching the maximum yields of 65.0 wt% and 68.7 wt% at 120 min, respectively (Fig. 3c and d). Meanwhile, the yield of glycolic acid were the maximum yield 16.6 wt% and 15.7 wt% for 12.5 and 20 g L^{-1} of starch, respectively.

According to Fig. 3, the conversion rate of starch degradation increased first and then decreased with the reaction time, whereas the conversion rate of starch degradation to monosaccharides gradually increases upon increasing the starch concentration. This is because PMo_{12} accelerated not only the acid hydrolysis of starch by the ionized H^+ but also the oxidation of the C–C bonds at higher concentrations of starch. As a result, organic acids such as glycolic acid and formic acid were generated, increasing the H^+ content in the reaction system and, in turn, the yield of monosaccharides. However, above a certain starch concentration, the reaction could not be completed at the beginning; thus, the yield of monosaccharides increased first. The initial increase in the yield of monosaccharide and the subsequent decrease can be explained in terms of the reaction sequence involving acid hydrolysis of starch to monosaccharide, followed by the conversion of the latter to highly active C_2 and C_4 products by retro-aldol reaction,²¹ which are then oxidized to acid by PMo_{12} . As the PMo_{12} catalyst is consumed, the oxidation reaction gradually weakens, resulting in a decrease in the yield of glycolic acid.

The products obtained using the four different starch concentrations were compared and analyzed. When the starch concentration was 2.5 g L^{-1} , the yield of glycolic acid in the products was the highest (22.5 wt%) at 240 min, whereas the total yield of monosaccharides and glycolic acid was 76.4 wt% at

120 min. However, this concentration of 2.5 g L^{-1} was equivalent to adding twice fresh water to the real wastewater sample, which contained a starch concentration of 5 g L^{-1} . For the latter concentration, the total yield of monosaccharides and glycolic acid reached 75.6 wt%. In contrast, at higher starch concentrations of 12.5 and 20 g L^{-1} , the starch could not be completely decomposed, and the yield of the product reached about 80.0 wt% only when the reaction time was further extended, implying more energy consumption. Therefore, the starch concentration was set to 5 g L^{-1} for the subsequent experiments.

3.3 Effect of the reaction temperature on the starch degradation products

The temperature of the reaction system is one of the important factors affecting the degradation of starch. The catalytic performance of PMo_{12} at $140 \text{ }^\circ\text{C}$, $145 \text{ }^\circ\text{C}$, $150 \text{ }^\circ\text{C}$, and $160 \text{ }^\circ\text{C}$ was evaluated according to the yield of monosaccharides and glycolic acid by setting the amount of PMo_{12} catalyst to 20 wt%, the concentration of starch to 5 g L^{-1} , and the reaction time to 60, 120, 180, 240, and 300 min. The results are shown in Fig. 4. When the reaction temperature was $140 \text{ }^\circ\text{C}$, the yield of monosaccharide and glycolic acid increased with the reaction time. However, the yield of monosaccharide increased first and then decreased, being the maximum yield 69.4 wt% at $145 \text{ }^\circ\text{C}$, whereas the yield of glycolic acid increased upon increasing the reaction time. When the reaction temperature was $150 \text{ }^\circ\text{C}$ and $160 \text{ }^\circ\text{C}$, the monosaccharide yield decreased with the increase of the reaction time due to the accelerated decomposition of monosaccharides at high temperature. A large number of C–O and C–C bonds in the structure were cleaved to form C_2 and C_4 small organic acids, and the condensation between monosaccharides to form first brown humins and then granular products was accelerated.³⁰ However, the yield of glycolic acid increased with the increase of temperature below $150 \text{ }^\circ\text{C}$. In contrast, a further increase of the reaction temperature produced a higher yield of glycolic acid (18.1 wt% at 60 min time) in the initial stage of reaction, and the degradation of organic compounds occurred with increasing the reaction time.

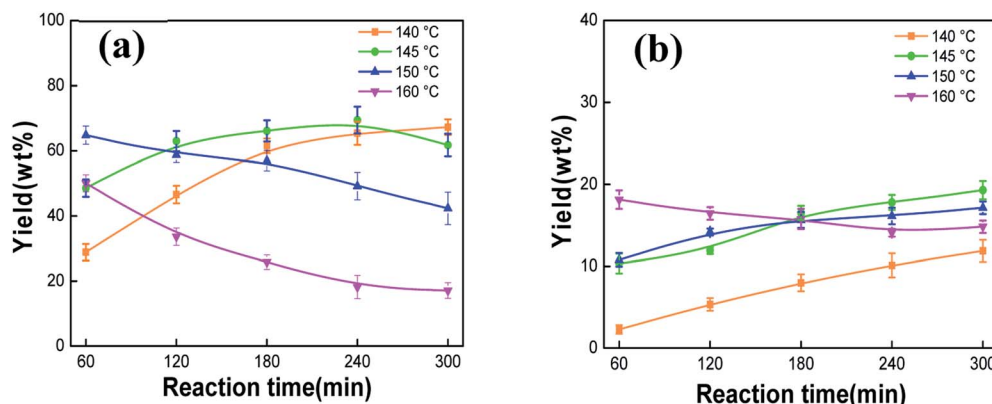


Fig. 4 Effect of the reaction temperature on the starch degradation products: (a) monosaccharide yield; (b) glycolic acid yield.



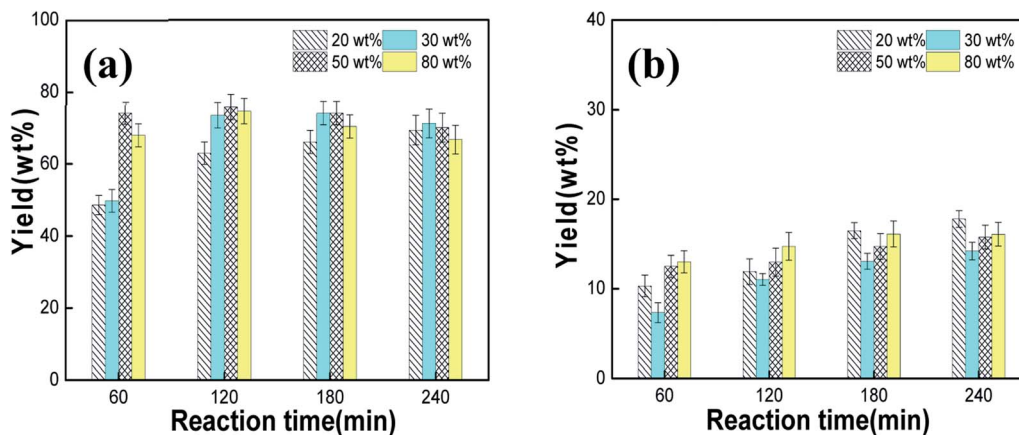


Fig. 5 Effect of the PMo₁₂ dosage on the starch degradation products: (a) monosaccharide yield; (b) glycolic acid yield.

The comparison of the catalytic oxidation of starch at four different temperatures shows that when the reaction temperature was 145 °C, not only the yield of monosaccharides and glycolic acid (87.2 wt% at 240 min) was high but also the ineffective degradation of starch at high temperature could be avoided. Therefore, the temperature of 145 °C was selected as the optimal reaction temperature.

3.4 Effect of the PMo₁₂ dosage on the starch degradation products

The acidity of PMo₁₂ could accelerate the hydrolysis of starch, and its oxidation ability was conducive to the cleavage of C–O bond and C–C bonds in the starch molecule, which was beneficial to the catalytic oxidation reaction. To study the effect of the amount of catalyst on the main products of starch degradation, the concentration of starch was fixed at 5 g L⁻¹ and the reaction temperature was set to 145 °C. As can be seen in Fig. 5a and b, the yield of monosaccharides and glycolic acid increased with the increase of the reaction time when using 20 wt% PMo₁₂. The yield of monosaccharides was 69.4 wt% and the yield of glycolic acid was 17.8 wt% at 240 min. When the amount of PMo₁₂ was increased to 30 wt%, the yields of monosaccharides and glycolic acid were

74.1 wt% and 13.1 wt% at 180 min, respectively. When the catalyst dosage was increased to 50 wt%, the yields of monosaccharides and glycolic acid reached 75.8 wt% and 13.0 wt% at 120 min, respectively. However, for an amount of PMo₁₂ of 80 wt%, similar yields of monosaccharides and glycolic acid were obtained (74.7 wt% and 14.8 wt% at 120 min, respectively).

The results revealed that the highest total yield of monosaccharides and glycolic acid was 87.2 wt% for a PMo₁₂ amount of 20 wt%, and an increase of the catalyst dosage increased the yield only slightly (87.2 wt%, 88.8 wt%, and 89.4 wt% for 30 wt%, 50 wt%, and 80 wt% PMo₁₂). Since these changes were not significant, the optimal amount of catalyst was set to 20 wt% from an economic point of view and theoretical data analysis.

3.5 Effect of the reaction solution pH on the starch degradation products

In the process of the acid hydrolysis of starch, pH is another important factor, since the concentration of H⁺ affects the degree and rate of starch hydrolysis. The yields of the main products of the PMo₁₂-catalyzed starch oxidation at pH values of the reaction system of 1, 2, 2.8, and 4 are shown in Fig. 6. At pH 1, the H⁺ concentration was higher in the reaction system, and

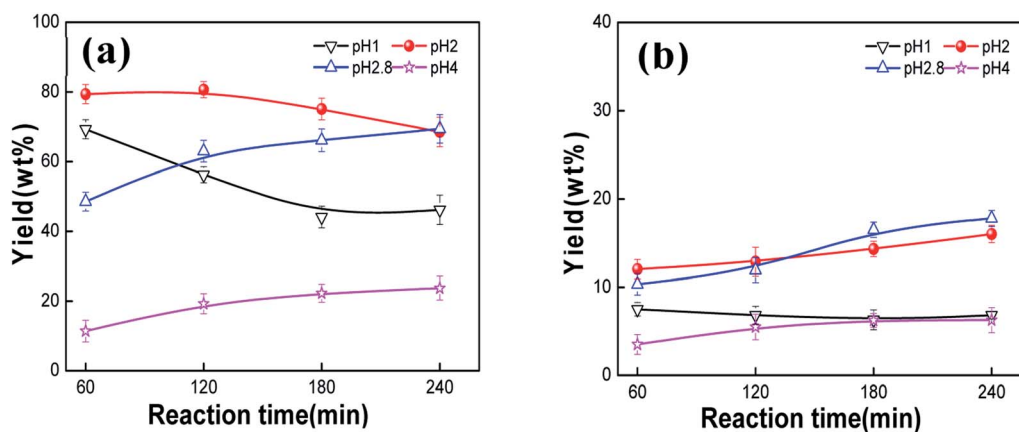
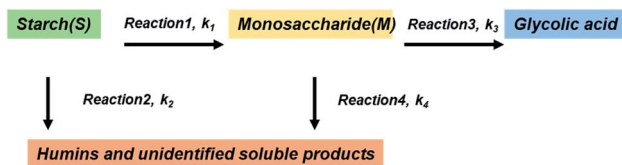


Fig. 6 Effect of pH on the starch degradation products: (a) monosaccharide yield; (b) glycolic acid yield.





Scheme 1 Kinetic model of starch conversion over.

the acid hydrolysis of starch was complete. The yield of monosaccharides reached 69.3 wt% at 60 min; however, it decreased gradually with the increase of the reaction time, reaching only 44.1 wt% at 180 min, and 19.6 wt% of levulinic acid was formed. When the pH of the reaction solution was 2, the yield of monosaccharides increased first and then decreased with the reaction time. Moreover, the yields of monosaccharides and glycolic acid were 80.7 wt% and 12.9 wt%, respectively, at 120 min. When the pH was 2.8, there was no additional acid, the monosaccharide yield still increased first and then decreased, but the maximum yield of 69.4 wt% was reached at 240 min, later than at pH 2. The yield of glycolic acid was 17.8 wt% at 240 min. At pH 4, the yields of monosaccharides and glycolic acid increased with the increase of the reaction time. However, when the reaction time was 240 min, the yields of monosaccharides and glycolic acid were only 23.7 wt% and 6.3 wt%, respectively, which were much lower than those obtained without adjusting the pH by adding NaOH.

The low pH value (high H^+ concentration) accelerated the hydrolysis of starch. A high monosaccharide yield was obtained at 60 min under pH 1. H^+ ions penetrated into the starch molecule in the hydrothermal reaction process, cleaving the α -1,4 and α -1,6 glycosidic bonds to form monosaccharide. Meanwhile, high reaction temperature and H^+ concentration promoted monosaccharide decomposing on account of the oxidation of PMO_{12} . It should be noted that the yield of monosaccharide at pH 2 was much higher than that at pH 1, 2.8 and 4. This was due to the fact that starch was hydrolyzed enough at pH value of 2, and H^+ concentration of pH 2 was insufficient to provide further degradation of starch. Therefore, pH 2 was beneficial to produce monosaccharide from starch. In contrast, the selective formation of glycolic acid was inhibited at high H^+ concentration, leading to the dehydration of glucose to produce 5-HMF. One molecule of levulinic acid and one of formic acid were produced by the decarboxylation of one molecule of 5-HMF under high temperature and acidic conditions. Therefore, the yield of levulinic acid reached 19.6 wt% at 180 min, which was much higher than that of glycolic acid. However, when the pH was adjusted to 2, the small addition of H^+ could promote the hydrolysis of starch to completion and reduce the formation of

byproducts and humins. When the pH was adjusted by adding NaOH, H^+ in the reaction system was consumed by OH^- , and the acidic hydrolysis of starch was inhibited. Although the selectivity of PMO_{12} to glycolic acid was still retained, the yield was lower than that under the previous conditions. Therefore, an appropriate addition of H^+ could promote the transformation of starch and reduce the formation of byproducts and humins.

3.6 Kinetic study for starch decomposition using phosphomolybdic acid

To the best of our knowledge, no kinetic study has been performed on the direct conversion of starch to glycolic acid. Although different products can be produced depending on the catalyst, PMO_{12} affords glycolic acid with high selectivity. Scheme 1 shows the reaction diagram used to construct the kinetic model of starch decomposition on the basis of the following four key steps comprising the starch conversion reaction: (1) the hydrolysis of starch to produce monosaccharides, (2) the degradation of starch to produce humins, (3) the retro-aldol reaction of the monosaccharides to produce glycolic acid, (4) and the degradation of the monosaccharides to produce humins.

According to the reaction diagram, the following rate differential eqn eqn (3)–(5) can be obtained:

$$-\frac{dC_S}{dt} = k_S C_S = (k_1 + k_2) C_S \quad (3)$$

$$\frac{dC_M}{dt} = k_1 C_S - k_M C_M = k_1 C_S - (k_3 + k_4) C_M \quad (4)$$

$$\frac{dC_{GA}}{dt} = k_3 C_M \quad (5)$$

where

$$k_S = k_1 + k_2 \quad (6)$$

$$k_M = k_3 + k_4 \quad (7)$$

The analytical expressions of the concentration of starch, monosaccharide, and glycolic acid were defined as eqn (8)–(10), respectively.

$$C_S = C_{S_0} e^{-k_S t} \quad (8)$$

$$\begin{aligned} C_M &= \frac{k_1 C_{S_0}}{k_M - k_S} (e^{-k_M t} - e^{-k_S t}) \\ &= \frac{k_1 C_{S_0}}{(k_3 + k_4) - (k_1 + k_2)} (e^{-k_3 t} - e^{-(k_1 + k_2) t}) \end{aligned} \quad (9)$$

$$\begin{aligned} C_{GA} &= \frac{k_1 k_3 C_{S_0}}{k_M - k_S} \frac{[k_M (1 - e^{-k_S t}) - k_S (1 - e^{-k_M t})]}{k_S k_M} = \frac{k_1 k_3 C_{S_0}}{(k_3 + k_4) - (k_1 + k_2)} \frac{[(k_3 + k_4)(1 - e^{-k_1 + k_2 t}) - (k_1 + k_2)(1 - e^{-(k_3 + k_4) t})]}{(k_1 + k_2)(k_3 + k_4)} \\ &= \frac{k_1 k_3 C_{S_0}}{(k_3 + k_4) - (k_1 + k_2)} \frac{[(k_3 + k_4)(1 - e^{-(k_1 + k_2) t}) - (k_1 + k_2)(1 - e^{-(k_3 + k_4) t})]}{(k_1 + k_2)(k_3 + k_4)} \end{aligned} \quad (10)$$



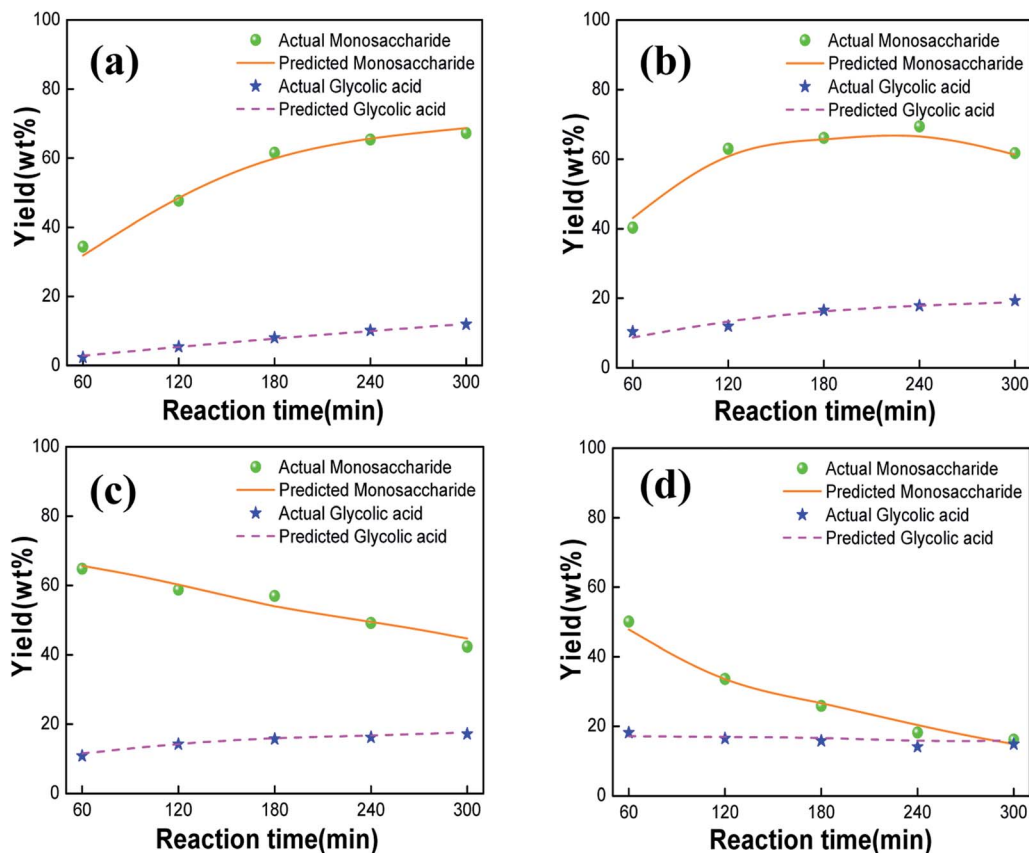


Fig. 7 Effect of the reaction temperature on the experimental and modeled concentration profiles: (a) 140 °C; (b) 145 °C; (c) 150 °C; (d) 160 °C.

In eqn (6)–(10), C_S , C_M , C_{GA} , and C_{S_0} are the concentration of starch, monosaccharide, and glycolic acid and the initial starch concentration, respectively. K_S , K_M , k_1 , k_2 , k_3 , and k_4 are the kinetic rate constants of starch decomposition, monosaccharide decomposition, reaction (1), reaction (2), reaction (3), and reaction (4), respectively. The reaction rate constants (k_1 , k_2 , k_3 , and k_4) of the kinetic study were calculated using eqn (9) and (10) using the MATLAB software and nonlinear least squares regression method. All experimental data were fitted by differential equations.

For general first-order chemical reactions, the relationship between reaction rate and temperature is in accordance with the Arrhenius equation (eqn (11) and (12)).

$$k = Ae^{-E_a/RT} \quad (11)$$

$$\ln k = \ln A - E_a/RT \quad (12)$$

where, A —pre-exponential factor, min^{-1} ; E_a —apparent activation energy, kJ mol^{-1} ; R —gas constant, $8.314 \text{ J (mol}^{-1} \text{ K}^{-1})$; T —temperature, K .

Generally, rate constants can be expected to depend on temperature. By fitting the parameters in eqn (8)–(10) using the MATLAB program,^{31,32} the resulting parameters were most consistent with the yield of monosaccharides and glycolic acid. Fig. 7 shows the predicted and experimental yields of monosaccharides and glycolic acid. The reaction rate constants, which were related to the reaction temperature of starch conversion to glycolic acid catalyzed by PMO_{12} , are shown in Table 2. It can be seen that the rate constant k_1 of starch decomposition increased with the increase of the temperature. In the reaction (2), the rate constant k_2 of starch conversion into

Table 2 Kinetic model first-order rate constants at four temperatures^a

T (°C)	k_1 (min^{-1})	k_2 (min^{-1})	k_3 (min^{-1})	k_4 (min^{-1})	RMSE
140	0.026	0.007	0.015	0.009	0.024
145	0.047	0.015	0.025	0.019	0.031
150	0.074	0.023	0.042	0.034	0.021
160	0.110	0.041	0.073	0.062	0.016

^a RMSE: Root Mean Squared Error.

Table 3 Kinetic model apparent activation energy and pre-exponential factor

Parameter	Reaction			
	1	2	3	4
E_a (kJ mol^{-1})	104.7	126.5	117.2	140.5
A (min^{-1})	7.1×10^{11}	3.6×10^{14}	1.6×10^{13}	9.7×10^{15}
R^2	0.94	0.95	0.98	0.96



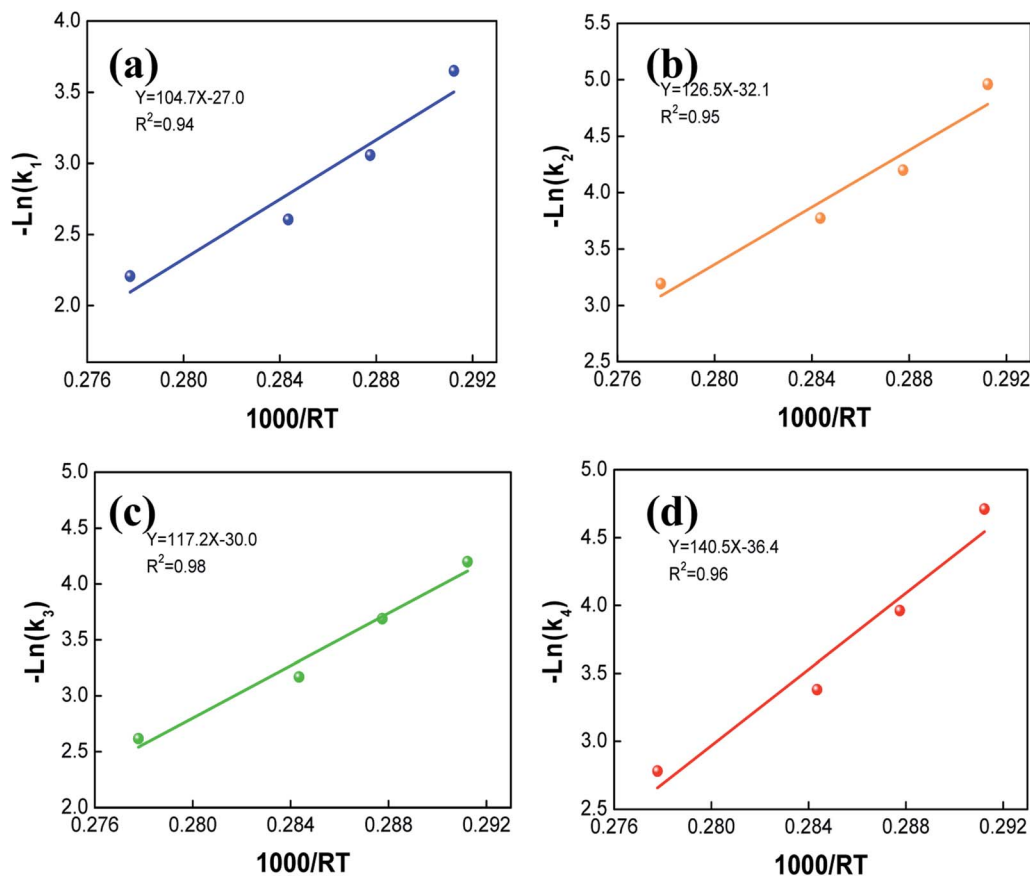


Fig. 8 Arrhenius plot of $-\ln(k)$ based on different temperature.

byproducts was smaller than k_1 , which indicates that starch was partly decomposed into humins. Therefore, the theoretical yield of glycolic acid could not be obtained from the starch conversion reaction. In the process of starch decomposition, the rate constant k_3 of reaction (3) was higher than that of reaction (4), which indicates that a high conversion of monosaccharides into glycolic acid was gotten. Root mean squared error (RMSE) is defined as the square root of the ratio of the deviation square between the predicted value and the true value and the number of observations n . It means that RMSE is the better when it is smaller.

The values of the apparent activation energy (E_a) and pre-exponential factor (A) for starch degradation catalyzed by PMo_{12} are listed in Table 3. These constants were fitted by the Arrhenius equation described in eqn (11) and (12). The intercept of the fitting curve represents the value of the pre-exponential factor (A), and the slope corresponds to the apparent activation energy, which were shown in Fig. 8. The E_a of reaction (1), (2), (3) and (4) were 104.7, 126.5, 117.2 and 140.5 kJ mol^{-1} , respectively. In the PMo_{12} catalytic system, the starch decomposition in reaction (1) and reaction (3) had lower apparent activation energy than that in reactions (2) and (4), indicating that the starch was inefficient degraded at high temperature. Moreover, humins were promoted at high temperatures from starch and monosaccharide.³³ Moreover, the

apparent activation energy for the monosaccharide conversion into glycolic acid was slightly higher than that of starch degradation to monosaccharide. In terms of economy and environment, a mild reaction temperature was important for producing glycolic acid, which could reduce the formation of humins.

4. Conclusions

The results herein presented show that WS from paper making process water could be converted into glycolic acid over PMo_{12} catalyst with high selectivity. Thus, the utilization of starch pollutants from the OCC pulping and papermaking process as a source of a high-value product was realized, and the micro-organism pollution problem in the papermaking process was solved. The catalytic oxidation of PMo_{12} to starch was a first-order reaction. The reaction rate constant increased with increasing the temperature, the apparent activation energy of starch to monosaccharide was 104.7 kJ mol^{-1} , the apparent activation energy of starch and monosaccharide to humins were 126.5 and 140.5 kJ mol^{-1} , and the apparent activation energy of monosaccharide to glycolic acid was 117.2 kJ mol^{-1} . When the reaction temperature was 145 °C, the reaction time was 120 min, and the pH of the reaction solution was 2, the yields of monosaccharides and glycolic acid were 80.7 wt% and 12.9 wt% respectively, which corresponds to a utilization of starch resources about 90.0 wt%. Therefore, this study demonstrates



the feasibility of the PMO_{12} -catalyzed oxidation and degradation of starch to produce high value-added glycolic acid, which has theoretical guiding significance and potential application value for the clean production and resource utilization of WS in the OCC papermaking process.

Conflicts of interest

The authors declare no competing financial interests.

Acknowledgements

The author thanks the support from the National Natural Science Foundation of China (No. 3177030417) and the Major Science and Technology Plan Project of Jiangsu Province (BE2018129). The authors also thank Yaoyao Liu for the modeling calculation.

References

- 1 F. d. A. C. Farias, M. M. d. S. Moretti, M. S. Costa, S. E. Bordignon Junior, K. B. Cavalcante, M. Boscolo, E. Gomes, C. M. L. Franco and R. d. Silva, *Ind. Crops Prod.*, 2020, **157**, 112825.
- 2 X. Li, C. Zhao, H. Zhang and W. Han, *Adv. Mater. Res.*, 2013, **848**, 321–324.
- 3 L. Lin, J. Yang, S. Ni, X. Wang, H. Bian and H. Dai, *J. Environ. Manage.*, 2020, **271**, 111031.
- 4 C. Association, *Pap. Biomater.*, 2020, 70–80.
- 5 P. K. Chatterjee, S. Neogi, S. Saha, B. H. Jeon and A. Dey, *Water Environ. Res.*, 2019, **91**, 377–385.
- 6 L. Sun, S. Wan, Z. Yu, Y. Wang and S. Wang, *Bioresour. Technol.*, 2011, **104**, 280–288.
- 7 Z. Zhang, O. Ortiz, R. Goyal and J. Kohn, *Princ. Tissue Eng.*, 2014, 441–473.
- 8 B. Mbituyimana, L. Mao, S. Hu, M. W. Ullah, K. Chen, L. Fu, W. Zhao, Z. Shi and G. Yang, *J. Bioresour. Bioprod.*, 2021, **6**, 129–141.
- 9 Y. D. Bello, A. P. Farina, M. A. Souza and D. Cecchin, *Mater. Sci. Eng., C*, 2020, **106**, 110283.
- 10 C. Chu, *Biotextiles as Medical Implants*, 2013, pp. 275–334.
- 11 J. Iglesias, I. Martínez-Salazar, P. Maireles-Torres, D. M. Alonso, R. Mariscal and M. L. Granados, *Chem. Soc. Rev.*, 2020, **49**, 5704–5771.
- 12 J. Zhang, X. Liu, M. Sun, X. Ma and Y. Han, *ACS Catal.*, 2012, **2**, 1698–1702.
- 13 G. Xu, A. Wang, J. Pang, X. Zhao, J. Xu, N. Lei, J. Wang, M. Zheng, J. Yin and T. Zhang, *ChemSusChem*, 2017, **10**, 1390–1394.
- 14 Z. She, J. Wang, J. Ni, X. Liu, R. Zhang, H. Na and J. Zhu, *RSC Adv.*, 2014, **5**, 5741–5744.
- 15 N. Candu, F. Anita, I. Podolean, B. Cojocaru, V. I. Parvulescu and S. M. Coman, *Green Process. Synth.*, 2017, **6**, 255–264.
- 16 C. Guarín, L. Gavilà, M. Constantí and F. Medina, *Chem. Eng. Sci.*, 2018, **179**, 83–91.
- 17 K. Guo, Q. Guan, J. Xu and W. Tan, *J. Bioresour. Bioprod.*, 2019, **4**, 202–213.
- 18 G. Yang, Y. Liu, K. Li, W. Liu, B. Yu and C. Hu, *Chin. Chem. Lett.*, 2020, **31**, 3233–3236.
- 19 G. Yang, D. Dilixiati, T. Yang, D. Liu, B. Yu and C. Hu, *Appl. Organomet. Chem.*, 2018, **32**, e4450.
- 20 A. A. Marianou, C. C. Michailof, D. Ipsakis, K. Triantafyllidis and A. A. Lappas, *Green Chem.*, 2019, **21**, 6161–6178.
- 21 A. Bayu, S. Karnjanakom, A. Yoshida, K. Kusakabe, A. Abudula and G. Q. Guan, *Catal. Today*, 2019, **332**, 28–34.
- 22 J. W. Lee, M. G. Ha, Y. B. Yi and C. H. Chung, *Carbohydr. Res.*, 2011, **346**, 177–182.
- 23 J. Tian, J. Wang, S. Zhao, C. Jiang, X. Zhang and X. Wang, *Cellulose*, 2010, **17**, 587–594.
- 24 W. Liu, W. Mu and Y. Deng, *Angew. Chem., Int. Ed.*, 2014, **53**, 13558–13562.
- 25 W. Deng, Q. Zhang and Y. Wang, *Dalton Trans.*, 2012, **41**, 9817–9831.
- 26 A. M. Khenkin and R. Neumann, *J. Am. Chem. Soc.*, 2008, **130**, 14474–14476.
- 27 I. K. M. Yu, D. Tsang, A. Yip, S. Chen, L. Wang, Y. S. Ok and C. S. Poon, *Bioresour. Technol.*, 2017, **237**, 222–230.
- 28 J. Horvat, B. Klaić, B. Metelko and V. Šunjić, *Tetrahedron Lett.*, 1985, **26**, 2111–2114.
- 29 N. Ya'aini, N. A. S. Amin and S. Endud, *Microporous Mesoporous Mater.*, 2013, **171**, 14–23.
- 30 W. Liu, Y. Cui, X. Du, Z. Zhang, Z. Chao and Y. Deng, *Energy Environ. Sci.*, 2016, **9**, 467–472.
- 31 A. Mukherjee and M. J. Dumont, *Ind. Eng. Chem. Res.*, 2016, **55**, 8941–8949.
- 32 W. Wei and S. Wu, *Chem. Eng. J.*, 2017, **307**, 389–398.
- 33 N. A. S. Ramli and N. A. S. Amin, *Chem. Eng. J.*, 2016, **283**, 150–159.

